analytical chemistry

ARTICLE

pubs.acs.org/ac

Universal Method for Determining Electrolyte Temperatures in Capillary Electrophoresis

Christopher J. Evenhuis, Michael U. Musheev, and Sergey N. Krylov*

Department of Chemistry and Centre for Research on Biomolecular Interactions, York University, Toronto, Ontario M3J 1P3, Canada

Supporting Information

ABSTRACT: Temperature increase in capillary electrophoresis (CE) due to Joule heating is an inherent limitation of this powerful separation technique. Active cooling systems can decrease the temperature of a large part of the capillary but they leave "hot spots" at the capillary ends which can completely ruin some CE analyses despite their short lengths. Here, we introduce a "universal method for determining electrolyte temperatures" (UMET) that can determine temperatures in both efficiently- and inefficiently-cooled parts of the capillary. UMET can be applied to all electrolytes, as it does not involve any probe; it requires only measuring current versus voltage for different voltages and processing the data using an iterative algorithm. To demonstrate the universality of UMET, we measured temperatures for electrolytes of different ionic strengths as well as for different capillary diameters. We further propose a "simplified universal method for predicting electrolyte temperatures" (SUMET) which only requires one measurement of current and voltage (that can be completed in 1 min) and uses two empirical equations to predict temperatures in the efficiently- and inefficiently-cooled parts of the capillary. The equations include several instrument-specific empirical parameters that are determined using a large set of current−voltage data obtained with UMET for a range of electrolytes and different capillaries. To demonstrate the utility of SUMET, we obtained the required data set for a Beckman MDQ CE instrument and produced all required empirical parameters that enable a user of this instrument to predict the temperature for every new experimental set in a matter of minutes. We confirmed the accuracy of SUMET by measuring the temperature-sensitive dissociation rate constant of a protein−DNA complex. We foresee that UMET will be used to produce instrument-specific empirical parameters for all CE instruments and then SUMET will be routinely used for temperature prediction in CE.

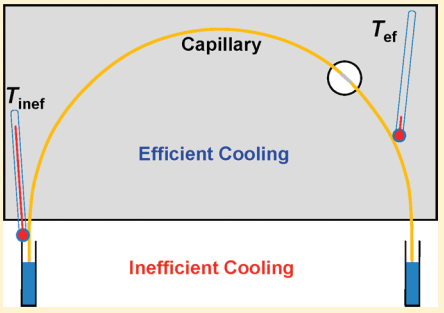

Joule heating, the resistive heating that occurs when an electric current is present in an electrolyte, has been recognized as a source of unwanted band broadening and decomposition of sensitive biological samples in capillary electrophoresis (CE) for several decades.[1−3] Various groups have measured and/or modeled the temperature increase inside capillaries that occur as a result of Joule heating.[3−18] To better control the temperature, commercial instruments are equipped with active cooling systems, where the major portion of the outer capillary wall is washed by a thermostat-controlled flow of liquid or air. There are, however, some inefficiently-cooled parts of the capillary that are sitting in the instrument interface or in ambient air. The difference in rates of heat removal from the surfaces of the efficiently- and inefficiently-cooled sections of the capillary leads to axial variations in the temperature of the electrolyte.[16,19−21] Xuan and Li made significant contributions in modeling end effects and axial temperature variations, which took into account the different cooling regimes experienced along the capillary. In spite of the fact that the axial temperature variations were previously acknowledged, the temperatures in both inefficiently- and efficiently-cooled regions of the capillary have never been experimentally determined.[15,16,21] Recently, our group showed that the inefficiently-cooled section of the capillary can have profound effects on the quantitative results of affinity analysis due to sample decomposition even when a low conductivity buffer in a standard capillary for CE was used.[22] Additionally, we were able to estimate the temperatures in the efficiently- and inefficiently-cooled regions by determining diffusion coefficients and by measuring rate constants for the dissociation of biomolecular complexes, respectively.[23] Unfortunately, the methods of temperature determination were experimentally challenging and time-consuming and had a low precision for measuring temperature in the inefficiently-cooled region.

We recently reported on heat-associated field distortion (HAFD) in electromigration systems with nonuniform heat-dissipation efficiencies.[24] We demonstrated the existence of HAFD through determining electric field strengths in efficiently- and inefficiently-cooled parts of a capillary in CE. Field determination was done through measurements of electric current at different voltages applied to the capillary and using an iterative algorithm of calculation. This work was motivated by an insight that a similar procedure can be used for the determination of

Received: December 8, 2010
Accepted: January 7, 2011
Published: February 02, 2011

temperatures in efficiently- and inefficiently-cooled parts of the capillary due to coupling between the electric field and temperature. We developed this idea into a universal method for determining electrolyte temperatures (UMET) in CE with active cooling systems. UMET can be applied to all electrolytes, as it does not involve any probe; it requires only measuring current versus voltage for different voltages and processing the data using an iterative algorithm. To demonstrate the universality of UMET, we measured temperatures for electrolytes of different ionic strengths as well as for different capillary diameters in a Beckman MDQ instrument. We also proposed a simplified UMET (SUMET) that requires only one current−voltage measurement that can be performed in a minute. SUMET also requires instrument-specific empirical parameters that can be collected once using UMET. We determined such parameters for a Beckman MDQ CE instrument which enables its users to predict the temperatures in the efficiently- and inefficiently-cooled regions of the capillary in a matter of minutes. We finally confirmed the accuracy of SUMET by comparing its data with those generated by UMET and also by measuring the temperature-sensitive dissociation rate constant of a protein−DNA complex for different capillary diameters and different temperatures of the coolant.

EXPERIMENTAL SECTION

Chemicals and Reagents. Thermostable DNA mismatch binding protein (MutS) from *Thermus aquaticus* was purchased from InterSciences (Markham, ON, Canada). A fluorescently labeled aptamer for MutS with the sequence 5′-/56-FAM/CTT CTG CCC GCC TCC TTC CGT CTT ATG TCG TTA GTC GCA GGG TGA TGA GTG AGG CAA GGG AGA CGA GAT AGG CGG ACA CT-3′ was synthesized by IDT (Coraville, USA). Analytical reagent grade sodium tetraborate, potassium choride, magnesium chloride, sodium acetate, sodium hydroxide, 35% w/w hydrochloric acid, glacial acetic acid, HPLC grade methano,l *Tris*(hydroxymethyl)aminomethane (TRIS), and TES (*N*-*Tris*(hydroxymethyl)methyl-2-aminoethanesulfonic acid) were purchased from Sigma Aldrich (Oakville, ON, Canada). All solutions were made using the Milli-Q-quality deionized water and filtered through a 0.22-μm filter (Millipore, Nepean, ON, Canada) system. The TRIS acetate buffer was prepared by dissolving TRIS and acetic acid in distilled water to produce a solution containing 50.0 mM TRIS and 25.0 mM CH_3COOH with a pH of 8.30. The process was repeated to produce the same buffer to which KCl was added to produce TRIS acetate buffers containing from 50 to 400 mM KCl. The buffer used for the determination of binding constants consisting of 50.0 mM TRIS and 25.0 mM CH_3COOH to which $MgCl_2$ was added to a concentration of 2.5 mM. Sodium tetraborate buffer with a pH of 9.20 was prepared by dissolving the salt in distilled water to make a 25.0 mM solution. TES buffer was prepared by dissolving the acid in distilled water and titrating it to a pH of 7.50 using a concentrated solution of NaOH. Approximately 0.1 M solutions of NaOH and HCl were prepared by dissolving the reagents in distilled H_2O.

Apparatus. All experiments were conducted using a Beckman Coulter MDQ P/ACE (Beckman Coulter, Oakville, Canada) instrument equipped with liquid cooling. Fused silica capillaries with internal diameters of approximately 20, 50, 75, 100, 150, 200, and 320 μm were purchased from Polymicro Industries (Phoenix, USA).

Electrophoretic Procedures. Before use, capillaries were rinsed by applying a pressure of 150 kPa for enough time to introduce 10 capillary volumes of methanol, 0.1 M HCl, 0.1 M NaOH, distilled H_2O, and the electrolyte in that order. Conductance measurements were made for each of the electrolytes by applying increments of 1 kV from 1 to 10 kV followed by increments of 2 kV from 10 to 30 kV for periods of 1 min at each voltage at a set temperature of 20 °C for capillary lengths of approximately 50 cm and internal diameters ranging from approximately 20 to 320 μm. Current and voltage data were collected at a frequency of 4 Hz. To evaluate the heat transfer coefficient for uncooled sections of the capillary, the liquid cooling system of the instrument was circumvented for capillary lengths of 50, 100, and 150 cm and conductance measurements were made at ambient temperature of ∼20 °C. Binding experiments between MutS and its aptamer were carried out at an electric field strength of 350 Vcm^{-1} using nonequilibrium capillary electrophoresis of equilibrium mixtures (NECEEM).[25] The equilibrium dissociation constant, K_d, and the rate constant of dissociation, k_{off}, were calculated using areas from NECEEM electropherograms as described in our previous publication.[26]

Data Processing and Analysis. The average values of the electric current and voltage were obtained by averaging the data from the last 50 s at each voltage and used to calculate experimental conductance for each voltage, G_{exp}:

$$G_{Exp} = \frac{I_{Exp}}{V} \quad (1)$$

where I_{Exp} and V are the electric current and voltage recorded by the instrument. Plots of G_{Exp} vs V were fitted using Origin software to find the conductance at the set temperature, G_0, the offset error in the electric current, I_0, and the autothermal parameter K_v for each capillary using the method described by Hruska et al.[20] The electric current values measured by the instrument were corrected by subtracting the offset error:

$$I = I_{Exp} - I_0 \quad (2)$$

The corrected electric current data was then used for the iterative process described in our previous manuscript to find refined values for V_{ef}, V_{inef}, ΔT_{ef}, ΔT_{inef}, $p_{L\ ef}$, and $p_{L\ inef}$.[24] The resulting values of ΔT_{ef} and ΔT_{inef} were plotted as a function of the average electric field strength, $E_{Average}$:

$$E_{Average} = \frac{V}{L} \quad (3)$$

where V is the applied voltage and L is the total length of the capillary.

The temperature coefficient of electrical conductivity, α, for each electrolyte was determined by collecting data at set temperatures of 15, 18, 20, 21, 24, 27, and 30 °C. A plot of $\kappa_0(T)$ vs T was interpolated to find κ_0(20 °C). The value of α was found by calculating the slope of a plot $\kappa_0(T)/\kappa_0$(20 °C) vs T. Details of the procedure are described in pS5 of the Supporting Information.

RESULTS AND DISCUSSION

Concept of UMET. As mentioned in our previous article, the capillary has one efficiently-cooled section and multiple sections which are inefficiently cooled (e.g., sections which are in contact with the electrolyte, room air, noncooled parts of the cassette which house the capillary or the detector interface).[22] To simplify the model, we assume that each of the inefficiently-cooled sections has similar heat removal efficiencies and we treat these

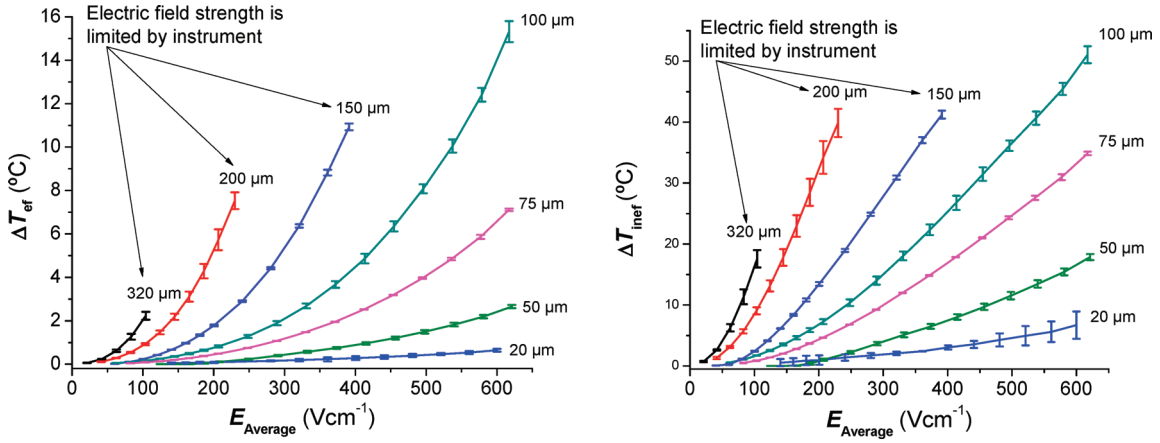

Figure 1. Variation of temperature increase, measured by UMET, for electrolyte in the efficiently-cooled (left panel) and inefficiently-cooled (right panel) sections of the capillary versus electric field strength for a range of internal diameters. Error bars show ±2 standard deviations ($n = 3$). The total length of each capillary was 48.6 cm, and the electrolyte was 100 mM TES adjusted to pH 7.5 with NaOH(aq). Before electrophoresis, buffer vials were kept at the same temperature as the set temperature of the capillary coolant.

regions as one. In our model, the capillary consists of just two sections: one that is inefficiently cooled and the other that is efficiently cooled. These behave like two resistors in series so that the current is constant throughout but the total voltage is equal to the sum of voltages in efficiently (V_{ef})- and inefficiently (V_{inef})-cooled regions:

$$V = V_{inef} + V_{ef} \tag{4}$$

The voltage in each section is directly proportional to its resistance, which in turn, is inversely proportional to the temperature of the electrolyte. As was demonstrated in our previous publication, the increase in temperature of the electrolyte in efficiently- and inefficiently-cooled regions can be described by the following equations:[24]

$$\begin{aligned} \Delta T_{ef} &= p_{L\ ef}\left(\frac{V_{ef}I}{L_{ef}}\right) = p_{L\ ef}E_{ef}I \\ \Delta T_{inef} &= p_{L\ inef}\left(\frac{V_{inef}I}{L_{inef}}\right) = p_{L\ inef}E_{inef}I \end{aligned} \tag{5}$$

where L_{ef} and L_{inef} are the lengths of the efficiently- and inefficiently-cooled regions, respectively. The coefficients $p_{L\ ef}$ and $p_{L\ inef}$ are constants that can be calculated using classical thermal theory for dissipation of heat energy from a heated cylinder:[5,9,12,20]

$$\begin{aligned} p_{L\ ef} &= \frac{1}{2\pi} \times \left[\frac{1}{4\lambda_{H_2O}} + \frac{1}{\lambda_{FS}}\ln\left(\frac{d_{FS}}{d_i}\right) + \frac{1}{\lambda_{PI}}\ln\left(\frac{d_o}{d_{FS}}\right) + \frac{2}{d_o h_{S\ ef}}\right] \\ p_{L\ inef} &= \frac{1}{2\pi} \times \left[\frac{1}{4\lambda_{H_2O}} + \frac{1}{\lambda_{FS}}\ln\left(\frac{d_{FS}}{d_i}\right) + \frac{1}{\lambda_{PI}}\ln\left(\frac{d_o}{d_{FS}}\right) + \frac{2}{d_o h_{S\ inef}}\right] \end{aligned} \tag{6}$$

where λ refers to the thermal conductivity, d to the diameter, h_S to the surface heat transfer coefficient, and the subscripts FS, PI, i, and o refer to fused silica, poly(imide), inner, and outer, respectively. For these calculations, the values of surface heat transfer coefficient for each section, $h_{S\ ef}$ and $h_{S\ inef}$, respectively are required. An estimate of $h_{S\ ef}$ was provided by the manufacturer: $h_{S\ ef}$ = 1136 $Wm^{2-}K^{-1}$, but it is not entirely clear whether this value applied to the efficiently-cooled part of the capillary or if it was an average value for the capillary as a whole.[27] By circumventing the instrument's cooling system altogether, we were able to use the approach of Hruska et al. to determine $h_{S\ inef} = 75 \pm 10\ Wm^{2-}K^{-1}$.[20,24] In most CE systems, the values of $h_{S\ ef}$ and $h_{S\ inef}$ are only known approximately, since they depend on the dimensions of the capillary, the ambient temperature inside the instrument, and the nature of the cooling system. Thus, to find more accurate values of $p_{L\ ef}$ and $p_{L\ inef}$, we used the iterative method described in our recent publication, which simultaneously determined the values of V_{ef}, V_{inef}, ΔT_{ef}, and ΔT_{inef}.[24] The accuracy of these values is determined by comparing the measured power produced by the instrument, VI with the total power calculated from each section, P_{inef} and P_{ef}:

$$x = \frac{P_{Measured}}{P_{inef} + P_{ef}} = \frac{VI}{V_{inef}I + V_{ef}I} \tag{7}$$

where x is a correction factor which adjusts ΔT_{ef} and ΔT_{inef} values and converges to 1 when accurate values of all parameters are obtained.

Universality of UMET. We applied UMET to find the temperature increase of a single electrolyte for a variety of capillaries differing in their internal diameter and, then, extended our investigation to include a range of electrolytes varying in electrical conductivity. Figure 1 shows the calculated temperature increases in the two regions of the capillary versus the average electric field strength for a range of internal diameters. The temperature increase in the efficiently-cooled region was much smaller than in the inefficiently-cooled region, as expected. For capillaries of larger internal diameter, it was not possible to determine the temperature over the same range of electric field strengths as the maximum electric field strength was restricted by the maximum current that was allowed to flow by the instrument. Figure 1 also illustrates that the assumption that temperature is well-controlled in the efficiently-cooled region is questionable, especially for capillaries with internal diameters exceeding 50 μm. This is important as capillaries with 75 or 100 μm internal diameters are widely used for temperature sensitive assays.[28,29]

To demonstrate the generic nature of UMET, we applied it to a single buffer but adjusted the ionic strength by adding varying amounts of KCl to adjust its conductivity. Figure 2 shows the influence of ionic strength on the temperature increases of the

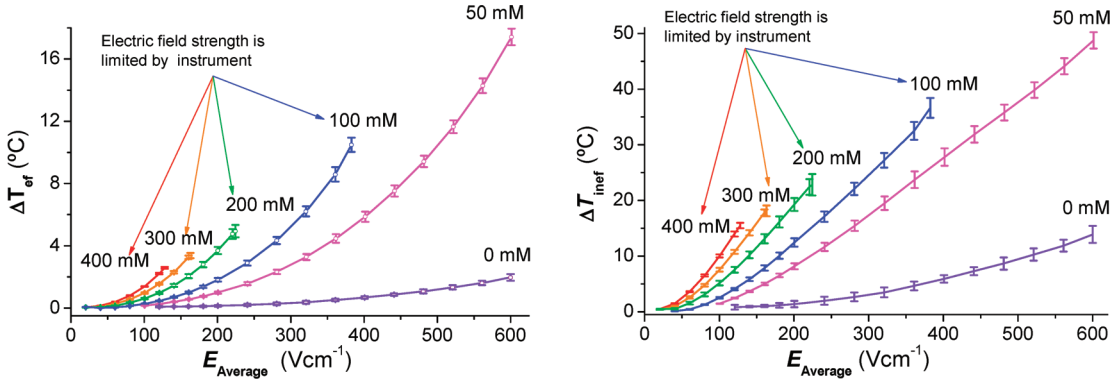

Figure 2. Variation of temperature increase for electrolyte in the efficiently-cooled (left panel) and inefficiently-cooled (right panel) sections of the capillary versus electrical field strength for a range of ionic strengths determined with UMET. Error bars show 2 standard deviations (n = 3). The total length of each capillary was 50.0 cm with an internal diameter of 75 μm. The electrolyte was 50 mM TRIS + 25 mM acetic acid, pH 8.3, to which varying concentrations of KCl were added. KCl concentrations are shown in the panels.

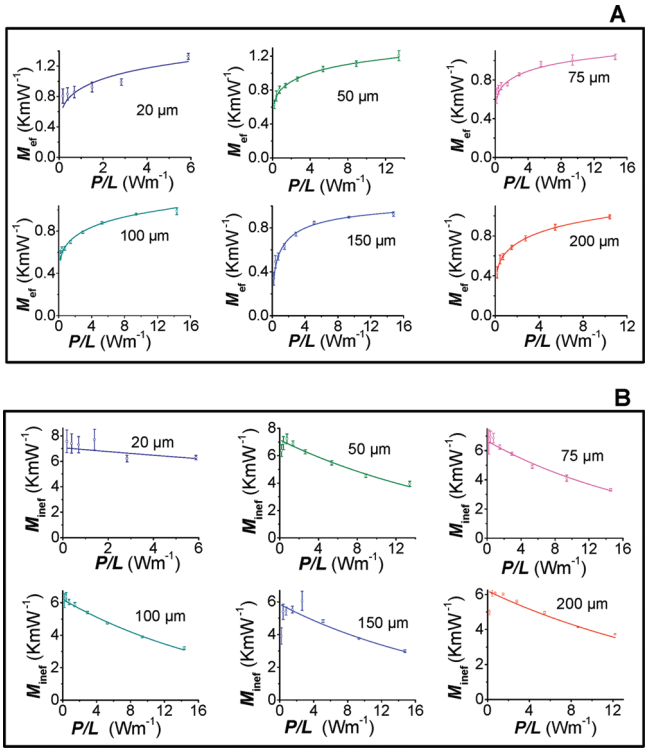

Figure 3. Universal multipliers for calculating the temperature rise in capillaries of variable internal diameter. Panel A shows how the multipliers vary with the power per unit length in the efficiently-cooled section of the capillary, and Panel B shows how they vary in the inefficiently-cooled sections. Error bars show ±2 standard deviations.

electrolyte vs electric field strength for a fixed internal diameter, d_i = 75 μm. As expected, for a particular electric field strength, the temperature increases in both the efficiently- and inefficiently-cooled sections of the capillary, become greater with the conductivity of the electrolyte. Practitioners may be tempted to assume that these significant temperature rises can be eliminated using capillaries with internal diameters of 50 μm or less; however, in practice, even in capillaries with 20 μm inner diameter, ΔT_{ef} and ΔT_{inef} may exceed 10 and 40 °C, respectively (see Figure S6 in Supporting Information), if $E_{Average}$ = 600 Vcm^{-1} and an electrolyte of sufficiently high conductivity ($\kappa \sim 5$ Sm^{-1}) is used.

Concept of SUMET. In practice, UMET is accurate and universal in nature but moderately time-consuming to implement. For each new electrolyte, the temperature coefficient for electrical conductivity, α, must first be determined. Obtaining reliable values of α requires multiple temperature-controlled experiments to be performed. Therefore, our next goal was to design simplified UMET (SUMET) that would require only a couple of minutes to do one short experiment and perform simple algebraic calculations. We hypothesized that the temperature increase in both efficiently- and inefficiently-cooled sections of the capillary should depend on the power per unit length averaged over the whole capillary:

$$\Delta T_{ef} = M_{ef}(V \times I)/L$$
$$\Delta T_{inef} = M_{inef}(V \times I)/L \quad (8)$$

where M_{ef} and M_{inef} are multipliers with units of KmW^{-1}. We further suggest that, since heat generation is not uniform throughout the capillary, the values of M_{ef} and M_{inef} are not constants but are functions of P/L. Testing our hypothesis required a large data set to be collected from a range of electrolytes and capillaries. We used UMET to collect the required data set (see Figures 1 and 2 as well as Figures S5−S16 in the Supporting Information). Except for the 20 μm capillary, the entire data set was used to determine the dependence of M_{ef} and M_{inef} on P/L (Figure 3). Fitting was problematic for low conductivity electrolytes in the 20 μm capillary due to the very small currents involved. Each of the plots of M_{ef} vs P/L were sigmoidal in shape, and the plots of M_{inef} vs P/L resembled exponential decay curves. Since analytical solutions for these dependences do not exist, we trialed a number of fitting functions using Origin software. The following equations gave us the best fits for our experimental data, M_{ef} and M_{inef} vs P/L:

$$M_{ef} = \frac{c\left(\frac{P}{L}\right)^n}{g + \left(\frac{P}{L}\right)^n}$$
$$M_{inef} = ka\left(\frac{P}{L}\right) \quad (9)$$

where c, g, n, k, and a are instrument-specific empirical parameters that are unique for each internal diameter (Tables 1 and 2). These

Table 1. Constants for Calculating M_{ef} for Capillaries of Varying Internal Diameters for a Beckman MDQ Instrument

d_i (μm)	c	g	n	R^2
20	20925	23064	0.186	0.7069
50	6203	7608	0.147	0.9953
75	6761	9066	0.129	0.9362
100	6583	9768	0.155	0.9759
150	1.108	0.883	0.593	0.9841
200	4.115	5.473	0.236	0.9979

Table 2. Constants for Calculating M_{inef} for Capillaries of Varying Internal Diameters for a Beckman MDQ Instrument

d_i (μm)	k	a	R^2
20	7.06	0.979	0.3238
50	7.16	0.953	0.9666
75	6.66	0.952	0.9855
100	6.22	0.952	0.9928
150	5.85	0.955	0.9236
200	6.21	0.955	0.9473

parameters describe the complex empirical functions which are derived from characterizing complex interplays of multiple processes. We did not anticipate meaningful trends in these parameters with respect to the inner diameter of the capillary, and we did not find such trends. These parameters serve a practical goal in temperature determination for a specific instrument and specific diameter of the capillary and should not be presumed to have any other importance.

The shapes of the plots in panels A and B of Figure 3 are not unexpected; as the rate of heat production increases, the power per unit length in the efficiently-cooled region increases and that in the inefficiently-cooled section decreases relative to the average value P/L. This explains the increase of M_{ef} and the decrease of M_{inef} as P/L increases.

Equations 8 and 9 and the parameters from Tables 1 and 2 allow an operator to predict ΔT_{ef} and ΔT_{inef} for any experiment conducted using a Beckmann CE instrument using only the experimental values of the currents and voltages recorded by the instrument. To test the stability of the predictions of ΔT_{ef}, we investigated the influences of variations in the efficiency of heat removal in the inefficiently-cooled section. Changing the value of $h_{S\ inef}$ by $\pm$20% caused the maximum variation of ΔT_{ef} of $\pm$ 0.1 °C. We also tested the influence of the temperature of the coolant on the values of M_{ef} and found that the effect was unnoticeable for the studied temperature range of 15−30 °C (see Figure S17 in the Supporting Information).

To demonstrate the accuracy of SUMET with respect to UMET, we predicted the temperature increase of an electrolyte that we had not used for the calibration graphs in Figure 3 but would be used in our final experiment. The electrolyte contained 50 mM TRIS, 25 mM CH_3COOH, and 2.5 mM $MgCl_2$. For an applied voltage of 30.0 kV in a 50.0 cm long capillary with d_i = 75 μm, the electric current was 64.5 μA and, thus, P/L = 3.87 Wm^{-1}. Substitution of P/L into eq 9 predicted M_{ef} = 0.887 KmW^{-1} and M_{inef} = 5.38 KmW^{-1}. By substituting these values into eq 8, we predicted ΔT_{ef} = 3.44 °C and ΔT_{inef} = 21.3 °C, in good agreement with the values determined using UMET for three consecutive experiments, ΔT_{ef} = 3.81 $\pm$ 0.08 °C and ΔT_{inef} = 22.1 $\pm$ 0.5 °C. For most practitioners, the differences between the values obtained for ΔT_{ef} and ΔT_{inef} from UMET and SUMET are insignificant. It should be emphasized that the parameters in Tables 1 and 2 are based on the results from several electrolytes so that the accuracy is not quite as good as using UMET for a single electrolyte of interest.

Test of UMET and SUMET. Finally, we used cross-verification to demonstrate the accuracy of our temperature predictions for capillaries of identical length but different internal diameters. First, we set the temperature of the coolant to be the same in both capillaries and rinsed them with the same electrolyte before applying the same average electric field strength. The resulting currents were used with eq 8 to predict the temperature of the electrolyte in the efficiently- and inefficiently-cooled section of each capillary. Next, by adjusting the temperature of the coolant for the capillary of the smaller internal diameter, we were able to mimic the temperature of the efficiently-cooled electrolyte in the larger bore capillary. To verify that the temperatures in the two capillaries were identical, we performed nonequilibrium capillary electrophoresis of equilibrium mixture (NECEEM) experiments using a temperature-sensitive biological model. If our predictions of the temperatures in both capillaries were accurate, we would expect the calculated kinetic parameters from each capillary to be the same.

As a model system, we used an equilibrium mixture of MutS protein and its fluorescently labeled DNA aptamer which has rate constants for association and dissociation of k_{on} and k_{off}, respectively:

$$\mathrm{MutS} + \mathrm{DNA} \underset{k_{of}}{\overset{k_{on}}{\rightleftharpoons}} \mathrm{MutS \cdot DNA}$$

We chose this model as the protein is thermo-stable and the values of k_{off} increase gradually with temperature until the aptamer melts and the complex completely dissociates. The melting temperature for the most thermodynamically stable aptamer structure is predicted to be 44.0 °C as per the IDT OligoAnalyser 3.1 program available at www.idtdna.com, but values for the 14 possible hairpin structures ranged from 37.0 to 49.3 °C.

We first performed experiments in the 75 and 150 μm capillaries with $E_{Average}$ = 350 Vcm^{-1} and the thermostat control set at 20 °C. In these experiments, the equilibrium mixture was moved past the inefficiently-cooled section using pressure as described elsewhere to avoid dissociation of the complex.[22] On the basis of the values of V_{tot} and I, we determined P/L for the 75 and 150 μm capillaries to be 1.22 and 4.55 Wm^{-1}, respectively. UMET predicted values of ΔT_{ef} to be 0.99 and 3.65 °C and values of ΔT_{inef} to be 8.52 and 20.9 °C, respectively. SUMET predicted values of ΔT_{ef} to be 0.93 and 3.71 °C and values of ΔT_{inef} to be 7.65 and 21.6 °C, respectively. To confirm the validity of our temperature predictions, we repeated the experiment in the 75 μm capillary with the temperature set at 22.6 °C so that the resulting temperature in the efficiently-cooled section with Joule heating would be ~23.6 °C, the same overall temperature as for the efficiently-cooled section of the 150 μm capillary with the temperature set at 20.0 °C. Finally, we performed the same experiment in the 150 μm capillary with the temperature control set at 20.0 °C but without moving the equilibrium mixture past the inefficiently-cooled section. We predicted that Joule heating in the inefficiently-cooled section would cause the temperature of the electrolyte to reach a temperature of ~41 °C. Figure 4 shows the NECEEM electropherograms from the

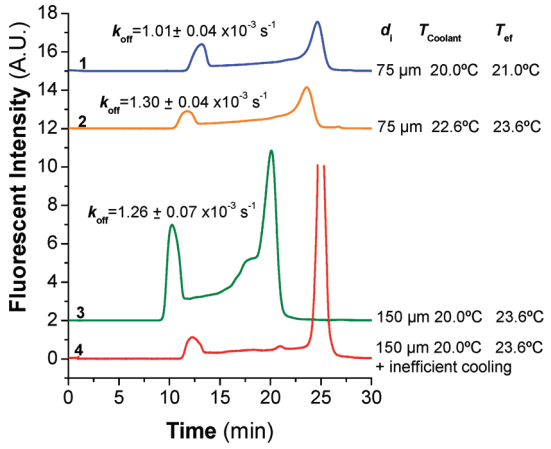

Figure 4. Influence of capillary diameter and temperature on the measurement of kinetic constants from NECEEM. Traces 1 and 2 correspond to separations in a 75 μm ID capillary with set temperatures of 20.0 and 22.6 °C, Trace 3 corresponds to the same separation as in 1 but in a 150 μm ID capillary. In traces 1−3, the equilibrium mixture was pushed into the efficiently-cooled part of the capillary by applying a low pressure pulse. For 1 and 2, p = 0.3 psi × 60 s, for 3, p = 0.014 psi × 600 s. The lower pressure was calculated from the difference in heights of the electrolytes in the inlet and outlet vials. Trace 4 illustrates the influence of the inefficiently-cooled section of the capillary. It had a maximum height of 36 arbitrary units but was truncated for clarity of presentation. The conditions were the same as for trace 3 except that the equilibrium mixture was not pushed into the efficiently-cooled section of the capillary prior to electrophoresis. The electrolyte used was 50 mM TRIS + 25 mM acetic acid + 2.5 mM $MgCl_2$. Sample injection was by pressure, p = 0.5 psi × 7 s for traces 1 and 2 and p = 0.1 psi × 16 s for traces 3 and 4. The electric field strength used for all separations was 350 Vcm^{-1}. Lengths of capillaries were identical for all separations. The concentrations of MutS protein and its aptamer in the injected equilibrium mixture were 100 and 50 nM, respectively. Standard errors for values of k_{off} and K_d are to ±2 standard deviations, n = 3 for d_i = 75 μm and n = 9 for d_i = 150 μm.

four experiments. The calculated k_{off} values from identical NECEEM experiments performed with the coolant temperature set at 20.0 °C in 75 and 150 μm capillaries were different (see Figure 4 traces 1 and 3). The increase in the complex dissociation in the larger diameter capillary was anticipated since Joule heating was expected to increase the electrolyte temperature in the efficiently-cooled region by an additional 2.8 °C. The calculated K_d values were similar (see Table S4 in Supporting Information for details) since they reflect the temperature of the original equilibrium mixture and are not affected by the separation conditions.[26] To validate our temperature predictions, we adjusted the set temperature of the coolant in the 75 μm capillary to mimic the temperature increased due to Joule heating in the 150 μm capillary (see Figure 4 trace 2). The effect of increasing the set temperature of the coolant by 2.6 °C was to increase the calculated values of k_{off} from 1.01 ± 0.04 × 10^{-3} s^{-1} to 1.30 ± 0.04 × 10^{-3} s^{-1}. The latter value is in excellent agreement with the k_{off} value of 1.26 ± 0.07 × 10^{-3} s^{-1} from the 150 μm capillary (see Figure 4 trace 3), confirming the validity of our predictions. Plot 4 shows the influence of the inefficiently-cooled section of the capillary on the equilibrium mixture. The fact that the peak for the complex was largely absent from the electropherogram suggests that the complex dissociated rapidly due to the increased temperature and a change to the conformation of the aptamer. These observations are consistent with our predictions that the temperature of the equilibrium mixture would approach the melting point of the aptamer in the inefficiently-cooled section of the capillary.

CONCLUSIONS

For any CE instrument for which the efficiency of heat removal is known, it is now possible to determine the rise in temperature of the electrolyte in both efficiently- and inefficiently-cooled regions of the capillary using only the voltage and current data accessible from the instrument. Our tables for calculating M_{ef} and M_{inef} in Beckmann CE instruments allow operators to predict the increase in temperature of the electrolyte in the efficiently- and inefficiently-cooled sections of the capillary with a precision typically within 5% of the measured value, irrespective of the electrolyte or internal diameter used. It should be noted that, for the rare cases when P/L < 0.1 Wm^{-1}, temperature determinations are less reliable due to the influence of larger uncertainties in conductivity that occur for low currents; needless to say, Joule heating is not problematic under such conditions. Our new tool for determining temperature allows operators to perform electrophoresis experiments in wider capillaries to those used normally without necessarily compromising separation efficiency. The unfavorable conditions in the inefficiently-cooled sections of the capillary can be avoided by moving the sample past the inefficiently-cooled section of the capillary before the separation voltage is applied. In large bore capillaries, the use of pressure to accomplish this may be unfavorable because the sample may be dispersed over a significant length of the capillary. This problem can be circumvented by performing an electrokinetic propagation of the sample using an electric field strength that is small enough not to overheat the sample. In this case, our temperature prediction tool will be invaluable for finding appropriate electrophoretic conditions for sample propagation.

ASSOCIATED CONTENT

Supporting Information. Experimental and theoretical sections. This material is available free of charge via the Internet at http://pubs.acs.org.

AUTHOR INFORMATION

Corresponding Author
*E-mail: skrylov@yorku.ca.

ACKNOWLEDGMENT

Funding for this research was generously provided by NSERC, Canada. A general annotated spreadsheet for temperature determination and detailed instructions for curve fitting of conductance vs voltage can be downloaded from the Research section of the following Web site: http://www.chem.yorku.ca/profs/krylov/.

REFERENCES

(1) Hjerten, S. *Chromatogr. Rev.* **1967**, *9*, 122–219.
(2) Knox, J. H. *Chromatographia* **1988**, *26*, 329–337.
(3) Nelson, R. J.; Paulus, A.; Cohen, A. S.; Guttman, A.; Karger, B. L. *J. Chromatogr.* **1989**, *480*, 111–127.
(4) Knox, J. H.; McCormack, K. A. *Chromatographia* **1994**, *38*, 215–221.

(5) Grushka, E.; McCormick, J. R. M.; Kirkland, J. J. *Anal. Chem.* **1989**, *61*, 241–246.
(6) Bello, M. S.; Righetti, P. G. *J. Chromatogr.* **1992**, *606*, 95–102.
(7) Vinther, A.; Soeberg, H. J. *J. Chromatogr.* **1991**, *559*, 27–42.
(8) Burgi, D. S.; Salomon, K.; Chien, R.-L. *J. Liq. Chromatogr.* **1991**, *14*, 847–867.
(9) Gobie, W. A.; Ivory, C. F. *J. Chromatogr.* **1990**, *516*, 191–210.
(10) Evenhuis, C. J.; Haddad, P. R. *Electrophoresis* **2009**, *30*, 897–909.
(11) Rathore, A. S. *J. Chromatogr., A* **2004**, *1037*, 431–443.
(12) Bello, M. S.; Chiari, M.; Nesi, M.; Righetti, P. G. *J. Chromatogr.* **1992**, *625*, 323–330.
(13) Bello, M. S.; Levin, E. I.; Righetti, P. G. *J. Chromatogr., A* **1993**, *652*, 329–336.
(14) Yu, L.; Davis, J. M. *Electrophoresis* **1995**, *16*, 2104–2120.
(15) Xuan, X.; Li, D. *J. Micromech. Microeng.* **2004**, *14*, 1171–1180.
(16) Xuan, X.; Li, D. *Electrophoresis* **2005**, *26*, 166–175.
(17) Berezovski, M.; Krylov, S. N. *Anal. Chem.* **2004**, *76*, 7114–7117.
(18) Musheev, M. U.; Javaherian, S.; Okhonin, V.; Krylov, S. N. *Anal. Chem.* **2008**, *80*, 6752–6757.
(19) Porras, S. P.; Marziali, E.; Gas, B.; Kenndler, E. *Electrophoresis* **2003**, *24*, 1553–1564.
(20) Hruska, V.; Evenhuis, C. J.; Guijt, R. M.; Macka, M.; Gas, B.; Marriott, P. J.; Haddad, P. R. *Electrophoresis* **2009**, *30*, 910–920.
(21) Xuan, X.; Sinton, D.; Li, D. *Heat Mass Transfer* **2004**, *47*, 3145–3157.
(22) Musheev, M. U.; Filiptsev, Y.; Krylov, S. N. *Anal. Chem.* **2010**, *82*, 8637–8641.
(23) Musheev, M. U.; Filiptsev, Y.; Krylov, S. N. *Anal. Chem.* **2010**, *82*, 8692–8695.
(24) Evenhuis, C. J.; Musheev, M. U.; Krylov, S. N. *Anal. Chem.* **2010**, *82*, 8398–8401.
(25) Berezovski, M.; Drabovich, A.; Krylova, S. M.; Musheev, M.; Okhonin, V.; Petrov, A.; Krylov, S. N. *J. Am. Chem. Soc.* **2005**, *127*, 3165–3171.
(26) Berezovski, M. V.; Krylov, S. N. *J. Am. Chem. Soc.* **2002**, *124*, 13674–13675.
(27) Bello, M. S.; Righetti, P. G. *J. Chromatogr.* **1992**, *606*, 103–111.
(28) Heegaard, N. H. H. *Electrophoresis* **2009**, *30*, S229–S239.
(29) Dolník, V. *Electrophoresis* **2006**, *27*, 126–141.

Supporting Information

Universal Method for Determining Electrolyte Temperature in Capillary Electrophoresis

Christopher J. Evenhuis, Michael U. Musheev, and Sergey N. Krylov

Department of Chemistry and Centre for Research on Biomolecular Interactions, York University, Toronto, Ontario M3J 1P3, Canada

Table of Contents

Calculation of the rise in temperature of the electrolyte when the power per unit length is 1 Wm^{-1} (finding the values of $p_{L\,ef}$ and $p_{L\,inef}$)

$p_{L\,ef}$ and $p_{L\,inef}$ are coefficients that relate the temperature increases of the electrolyte in each section of the capillary, ΔT_{ef} and ΔT_{inef}, to the local rate of heat production, P/L_{ef} and P/L_{inef}, respectively:

$$\Delta T_{ef} = p_{L\,ef}\left(\frac{P}{L}\right)_{ef}$$
$$\Delta T_{inef} = p_{L\,inef}\left(\frac{P}{L}\right)_{inef} \quad \text{(S1)}$$

where $p_{L\,ef}$ and $p_{L\,inef}$ are constants measured in KmW^{-1}, P is the rate at which heat energy is generated in watts and L is the capillary length in metres. The constants, $p_{L\,ef}$ and $p_{L\,inef}$ vary inversely with the surface heat transfer coefficients for the efficiently-cooled and inefficiently-cooled sections of the capillary, $h_{S\,ef}$ and $h_{S\,inef}$ respectively. The surface heat transfer coefficients measures the rate of heat removal from a unit of area by a coolant in contact with the surface when their temperatures differ by 1 K. h_S has units of $Wm^{-2}K^{-1}$. For a Beckman Coulter MDQ P/ACE instrument equipped with liquid cooling, the value of $h_{S\,ef}$ quoted by the manufacturers is 1136 $Wm^{-2}K^{-1}$. Our previous studies suggested that $h_{S\,inef}$ = 75 $Wm^{-2}K^{-1}$.[1] This valued agreed well with published values.[2-4] Applying classical theory of heat removal from a cylinder to a poly(imide) coated fused silica capillary containing an aqueous buffer, it is possible to write an expression for $p_{L\,ef}$ and $p_{L\,inef}$:[5]

$$p_{L\,ef} = \frac{1}{2\pi}\left[\frac{1}{4\lambda_{H_2O}} + \frac{1}{\lambda_{FS}}\ln\left(\frac{d_{FS}}{d_i}\right) + \frac{1}{\lambda_{PI}}\ln\left(\frac{d_o}{d_{FS}}\right)\right] + \frac{1}{\pi d_o h_{S\,ef}}$$
$$p_{L\,inef} = \frac{1}{2\pi}\left[\frac{1}{4\lambda_{H_2O}} + \frac{1}{\lambda_{FS}}\ln\left(\frac{d_{FS}}{d_i}\right) + \frac{1}{\lambda_{PI}}\ln\left(\frac{d_o}{d_{FS}}\right)\right] + \frac{1}{\pi d_o h_{S\,inef}} \quad \text{(S2)}$$

where λ is the thermal conductivity and d refers to the diameter. The subscripts: FS, i, PI, and o refer to fused silica, internal, poly(imide) and outer, respectively. At 20 ºC, the values of the constants are λ_{H_2O} = 0.5984 $Wm^{-1}K^{-1}$, λ_{FS} = 1.40 $Wm^{-1}K^{-1}$, and λ_{PI} = 0.155 $Wm^{-1}K^{-1}$.[5]

Most fused silica poly(imide) coated capillaries used for capillary electrophoresis have an outer diameter of $d_o \sim 360$ µm, a fused silica diameter of $d_{FS} \sim 320$ µm and variable internal diameter from d_i = 20 – 200 µm. By substituting each of these values into Eq. (S2), we obtain the simplified expression:

$$p_L = (0.241 - 0.503)\ KmW^{-1} + \frac{884.2\ m^{-1}}{h_S} \quad \text{(S3)}$$

p_L tends to be larger in smaller internal diameter capillaries than for larger internal diameter capillaries as in smaller internal diameter capillaries, there is a larger thickness of fused silica through which heat energy is conducted.

Table S1: Calculated values of $p_{L\ ef}$ and $p_{L\ inef}$ for standard poly(imide) coated capillaries with dimensions d_o = 360 µm and d_{FS} =320 µm with variable internal diameter based on Eq. 5 in the main text.

Internal Diameter (µm)	20	25	50	75	100	150	200
$p_{L\ ef}$ (KmW^{-1}) for $h_{S\ ef}$ = 1136 $Wm^{-2}K^{-1}$	1.281	1.256	1.177	1.131	1.098	1.052	1.019
$p_{L\ ef}$ (KmW^{-1}) for $h_{S\ ef}$ = 566 $Wm^{-2}K^{-1}$	2.065	2.039	1.961	1.915	1.882	1.836	1.803
$p_{L\ inef}$ (KmW^{-1}) for $h_{S\ inef}$ = 75 $Wm^{-2}K^{-1}$	12.29	12.27	12.19	12.14	12.11	12.06	12.03

Table S1 shows the influence of the size of the surface heat transfer coefficient on the temperature rise of the electrolyte when the heating power per unit length, P/L = 1.0 Wm^{-1}. The higher is the surface heat transfer coefficient and the thinner the walls of the capillary, the smaller is the increase in temperature of the electrolyte. The three values of the surface heat transfer coefficient used in the table correspond to: liquid cooling in a Beckman Coulter MDQ P/ACE instrument, cooling using a stream of air with a velocity of 10 ms^{-1} as employed in Agilent CE instruments and passive cooling in which there is no flow of fluid around the capillary.

Table 2 gives the corresponding values for AF-Teflon® coated capillaries. AF Teflon has a thermal conductivity of 0.116 $Wm^{-1}K^{-1}$.[6] Comparison of **Tables 1** and **2** shows that by virtue of their thinner wall coating, Teflon® coated capillaries have slightly better heat dissipation properties than poly(imide) coated capillaries despite Teflon's lower thermal conductivity.

Table 2: Predicted coefficients for AF-Teflon® coated capillaries with dimensions d_o = 363 µm and d_{FS} = 333 µm with variable internal diameter based on Eq. 5 in the main text.

Internal Diameter (µm)	50	75	100
$p_{L\ ef}$ (KmW^{-1}) for $h_{S\ ef}$ = 1136 $Wm^{-2}K^{-1}$	1.172	1.126	1.094
$p_{L\ ef}$ (KmW^{-1}) for $h_{S\ ef}$ = 566 $Wm^{-2}K^{-1}$	1.950	1.904	1.871
$p_{L\ inef}$ (KmW^{-1}) for $h_{S\ inef}$ = 75 $Wm^{-2}K^{-1}$	12.09	12.05	12.01

Estimation of ΔT_{ef} and ΔT_{inef}

As a first order approximation, Equation (S4) and values from **Table 1** can be used to estimate the rise in temperature of the electrolyte in the efficiently- and inefficiently cooled sections of the capillary:

$$\Delta T_{ef} = p_{L\ ef}\left(\frac{VI}{L}\right)$$
$$\Delta T_{inef} = p_{L\ inef}\left(\frac{VI}{L}\right) \quad \textbf{(S4)}$$

This approximation underestimates the temperature rise of the electrolyte in the efficiently cooled section of the capillary and overestimates the temperature rise in the inefficiently cooled section as the electric field strength is not uniform throughout but significantly weaker $E_{Average}$ in the inefficiently cooled section and slightly stronger than $E_{Average}$ in the efficiently cooled section.

Finding the conductivity of the electrolyte at the ambient temperature, κ_0

The iterative process for accurately determining the temperature of the electrolyte in each section of the capillary relies heavily on knowing the conductivity of the electrolyte at the ambient temperature, κ_0 and on how the conductivity changes with temperature. κ_0, can be determined from the conductance at ambient temperature, G_0. Conductance, G, is the reciprocal of resistance:

$$G = \frac{I}{V} \tag{S5}$$

where I is the electric current that flows in an electrolyte when a voltage, V, is applied across it.

$$\kappa_0 = \frac{G_0 L}{A} = \frac{4 G_0 L}{\pi d_i^{\,2}} \tag{S6}$$

In Equation (S6), A is the internal cross-sectional area of the electrolyte.

Determining the conductance free of Joule heating, G_0. For a perfectly functioning instrument with no systematic error in measurement of the current and a uniform cooling efficiency for the entire capillary, the conductance of the electrolyte within the capillary is expected to increase with the applied voltage as shown below: [7]

$$G(V) = \frac{G_0}{1 - K_V V^2} \tag{S7}$$

where $G(V)$ is the conductance of the solution as a function of the voltage, V, G_0 is the conductance in the absence of an electrical field, and K_v is the autothermal parameter (V^{-2}). According to Eq. (S7) G is expected to increase smoothly with V from a value of G_0 at $V = 0$. In practice, this is never observed; instead there is an initial decrease in G with increasing V. **Figure S1** shows a typical plot of experimentally determined conductance versus voltage.

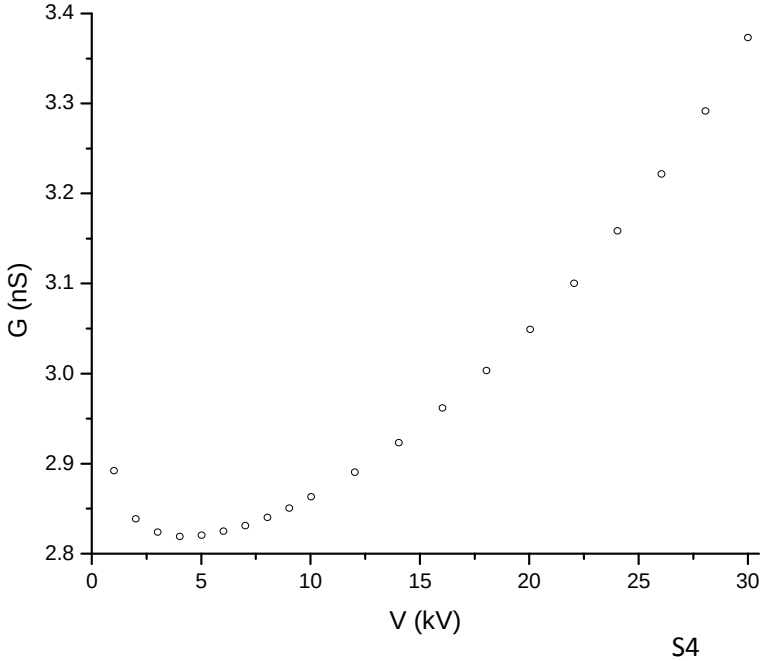

Figure S1: Plot of Experimental Conductance versus Voltage for a 50 cm long, 75 µm capillary containing 100 mM TES buffered to a pH of 7.50 using NaOH(aq). The thermostat for cooling was set at 20.0ºC.

Hruska *et al.* explained the discrepancy in conductance by postulating that there is a systematic error in measurement of the electric current; which they referred to as a current offset error, I_0.[7]

$$I_{\text{exp}} = I_0 + I \qquad \textbf{(S8)}$$

where I_{exp} is the current measured by the instrument and I is the actual current. It follows that any measurement of conductance is influenced by this systematic error in the instrument measured electric current.

$$G_{\text{exp}}(V) = \frac{I_0}{V} + \frac{G_0}{1 - K_{\text{V}} V^2} \qquad \text{(S9)}$$

where $G_{\text{exp}}(V)$ is the experimentally determined conductance. **Figure S1** shows that the influence of the offset error is the greatest at low voltages. This is to be expected as the error in the conductance, I_0/V increases as $V \rightarrow 0$.

Figure S2 demonstrates that the parameters I_0, G_0 and K_{V} can be determined by curve fitting of Equation (S9) using suitable software. Following fitting, Eq. (S6) allows the conductivity at the ambient temperature, κ_0, to be calculated from G_0. Notice that the fitted value for $G_0 < G_{\text{Exp}}$ for all values of V.

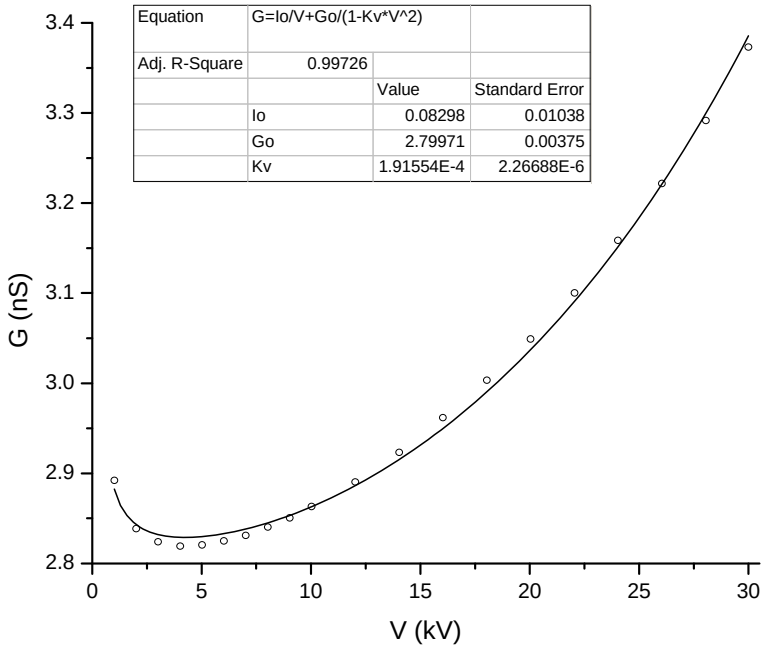

Figure S2: Fitting of experimental conductance versus voltage to (Eq. S9).The conditions are identical to those shown in **Figure S1**

Finding the temperature coefficient of conductivity, α

Conductivity increases linearly with temperature.

$$\kappa = \kappa_0 (1 + \alpha \Delta T) \qquad \textbf{(S10)}$$

As κ_0 is the conductivity free from Joule heating effects, α can be determined by collecting κ_0 data for a range of set temperatures and plotting a graph of κ/κ_0 *vs* ΔT where ΔT is the difference between the actual temperature and the reference temperature:

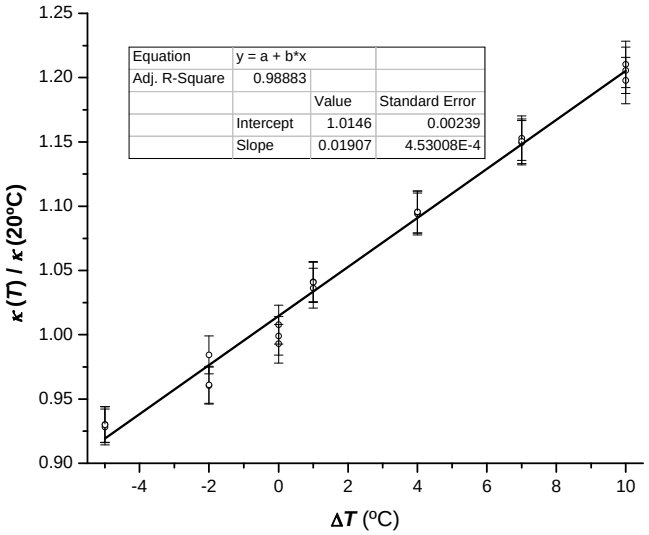

Figure S3: Variation of conductivity with Temperature for electrolyte containing 50 mM TRIS, 25 mM Acetic Acid and 300 mM KCl. Conductivities were calculated from G_o values determined at set cooling temperatures of 15, 18, 21, 24, 27, and 30ºC. Each measurement was performed three times in a 49.9 cm long capillary with an internal diameter of 75 µm. Error bars show ± 2 standard deviations and calculated standard errors are for the 95% confidence interval.

$$\alpha = \frac{\kappa - \kappa_0}{\kappa_0 \Delta T} \qquad \textbf{(}S11\textbf{)}$$

Figure S3 shows how the quotient $\kappa_0/\kappa_0(20.0ºC)$ varies with ΔT = T – 20.0ºC. The temperature coefficient of conductivity was determined from the slope of this graph; $\gamma = 0.01907 \pm 0.00045$ K^{-1}.

Table 3: Temperature coefficients of electrical conductivity used for buffers. Values with a single * were interpolated and those with **extrapolated.

Buffer composition	**$\alpha \pm$ standard error (K^{-1})**
10 mM TRIS + 10 mM HCl	0.01825 ± 0.00059
50 mM TRIS + 25 mM CH_3COOH	0.02221 ± 0.00048
25 mM CH_3COOH + 25 mM $NaCH_3COO$	0.02033 ± 0.00007
25 mM $Na_2B_4O_7$	0.02183 ± 0.00026
100 mM TES +*x* mM NaOH (pH 7.5)	0.02093 ± 0.00021
50 mM TRIS + 20 mM HCl + 2.5 mM $MgCl_2$ + 5 mM KCl	0.01992 ± 0.00024

50 mM TRIS + 25 mM CH_3COOH + 2.5 mM $MgCl_2$	0.02210± 0.00028
50 mM TRIS + 25 mM CH_3COOH + 50 mM KCl	0.01959 ± 0.00032
50 mM TRIS + 25 mM CH_3COOH + 100 mM KCl	0.0195* ± 0.0004
50 mM TRIS + 25 mM CH_3COOH + 200 mM KCl	0.01976 ± 0.00019
50 mM TRIS + 25 mM CH_3COOH + 300 mM KCl	0.01907 ± 0.00047
50 mM TRIS + 25 mM CH_3COOH + 400 mM KCl	0.0185** ± 0.0005

Refining estimates of the temperature increase in each section of the capillary

As a first approximation Eq. (S4) is used to find ΔT_{ef} and ΔT_{inef} These temperature increases are used to calculate the electrical conductivities of the electrolyte in each section using the following equation:

$$\kappa_{ef} = \kappa_0(1 + \alpha\Delta T_{ef})$$
$$\kappa_{inef} = \kappa_0(1 + \alpha\Delta T_{inef}) \quad \text{(S12)}$$

It may be shown that the electrical field strength in each section is given by Eq. (S13). A complete derivation is given in our previous article:[1]

$$E_{ef} = \frac{\kappa_{inef} V}{\kappa_{inef} L_{ef} + \kappa_{ef} L_{inef}}$$
$$E_{inef} = \frac{\kappa_{ef} V}{\kappa_{inef} L_{ef} + \kappa_{ef} L_{inef}} \quad \text{(S13)}$$

As $\kappa_{inef} > \kappa_{inef}$, it follows that $E_{ef} > E_{Average}$ and that $E_{inef} < E_{Average}$. The initial estimates of conductivity from Eq (S12) are used to refine the electrical field strength in each section.

The refined estimates of the electrical field in each section are used to recalculate the power per unit length in each section using the following equation:

$$\left(\frac{P}{L}\right)_{ef} = E_{ef} I$$
$$\left(\frac{P}{L}\right)_{inef} = E_{inef} I \quad \text{(S14)}$$

An improved estimate of the temperature increases in each section is obtained by using these new power per unit lengths in Eq. (S1):

$$\Delta T_{ef} = p_{L\,ef} E_{ef} I$$
$$\Delta T_{inef} = p_{L\,inef} E_{inef} I \quad \text{(S15)}$$

To know how accurate these estimates are, the calculated total heating power is compared with the measured heating power using the voltage and current readings from the instrument:

$$P_{Calculated} = L_{ef} E_{ef} I + L_{inef} E_{inef} I \quad \text{(S16)}$$

$$P_{\text{Measured}} = VI \tag{S17}$$

$$x = \frac{P_{\text{Measured}}}{P_{Calculated}} \tag{S18}$$

The factor x is used to adjust the temperature estimates before recalculating κ, E and P/L in each section during the next iteration. This process is repeated until x converges to 1. This iterative process works well when $P/L \geq 0.1$ Wm^{-1}, but at lower power per unit lengths, x may not converge due to the uncertainty in the offset current, I_0.

The steps described in Eqs. (S12- S18) are shown in the flowchart below. Note that the 3rd and subsequent iterative steps are different to previous steps in that the temperature is adjusted by the factor x after each iteration.

$$\Delta T_{i+1} = x_i \Delta T_i \tag{S19}$$

Iteration is continued until the desired convergence is observed. The value of "Min" determines the number of significant figures. For example if "Min" = 10^{-4}, only the fifth significant figure in the temperature will change through further iterations.

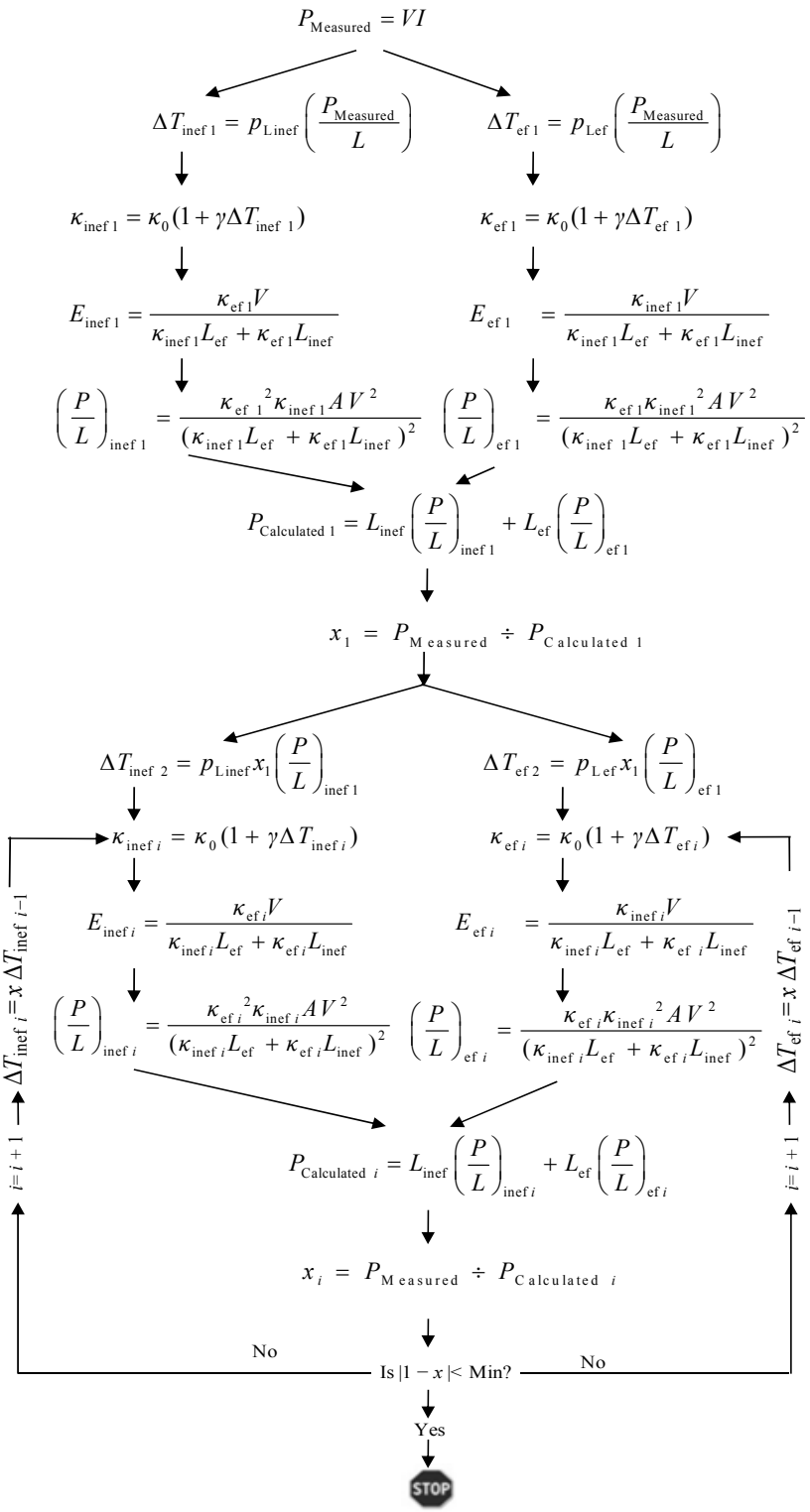

Figure S4: Flowchart for refining the estimates of the temperature increase in each section of the capillary at each voltage. "Min" is a parameter which determines how many iterations are required. The number of decimal places in "Min" determines the number of significant figures in the estimates of κ, E, P/L, and ΔT.

Collated data for capillaries of varying internal diameters containing a range of electrolytes

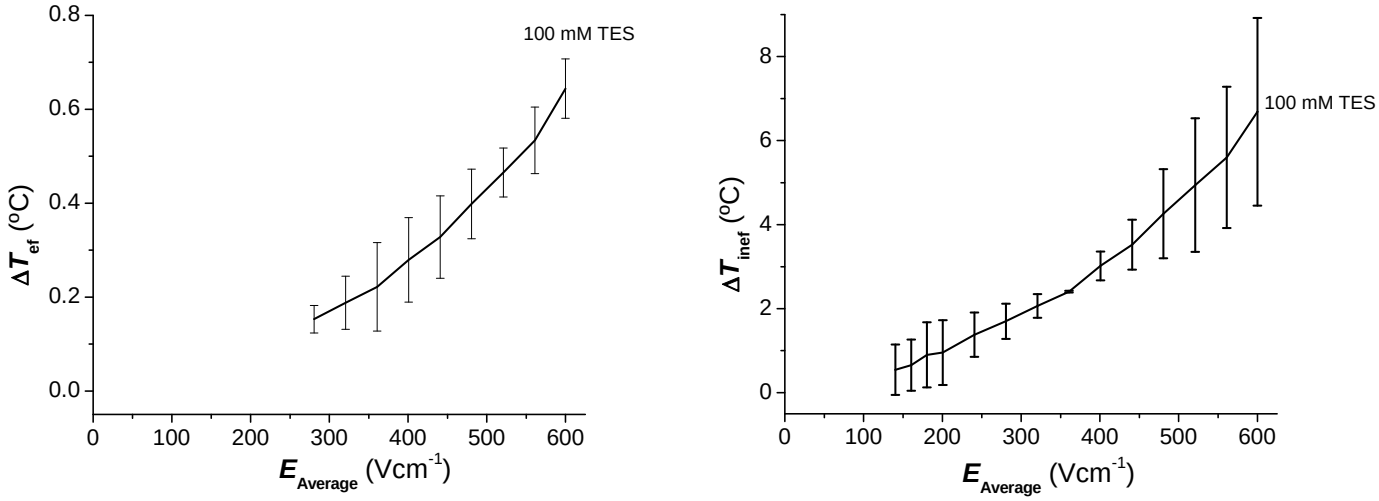

Figure S5: Increase in temperature as a function of the electric field strength in the efficiently-cooled section (**Left**) and inefficiently-cooled section (**Right**) of a 20 µm internal diameter capillary containing 100 mM TES electrolyte with the coolant temperature set to 20ºC. Error bars are to ± 2 standard deviations.

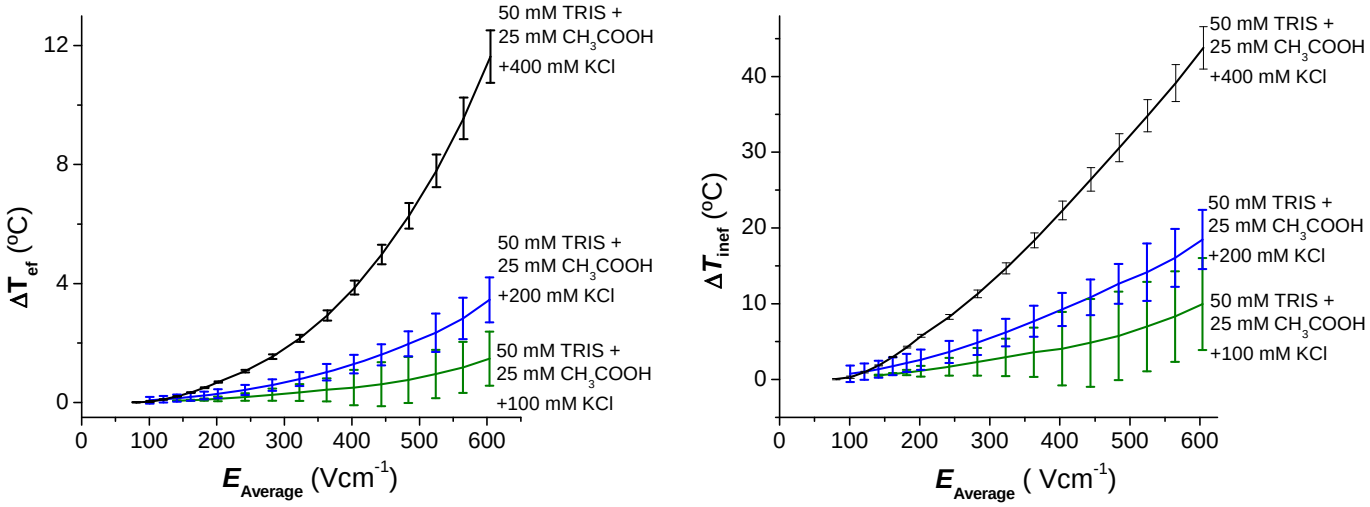

Figure S6: Increase in temperature as a function of the electric field strength in the efficiently-cooled section (**Left**) and inefficiently-cooled section (**Right**) of a 20 µm internal diameter capillary containing 50 mM TRIS + 25 mM CH_3COOH with varying concentration s of KCl. The coolant temperature was set to 20ºC. Error bars are to ± 2 standard deviations.

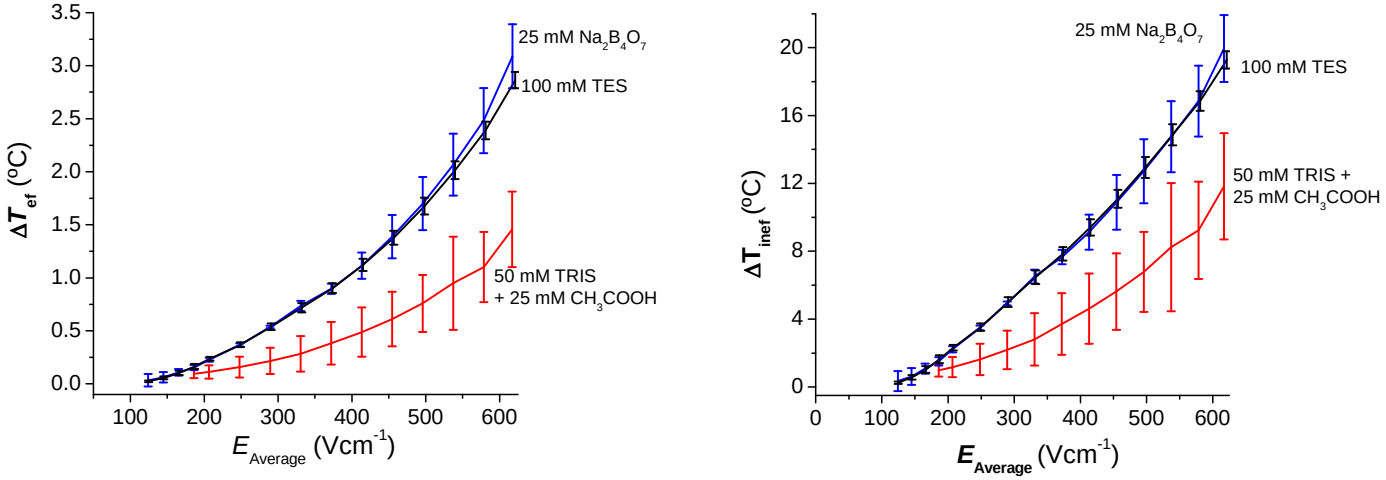

Figure S7: Increase in temperature as a function of the electric field strength in the efficiently-cooled section (**Left**) and inefficiently-cooled section (**Right**) of a 50 µm internal diameter capillary containing various electrolytes. The coolant temperature was set to 20ºC. Error bars are to ± 2 standard deviations.

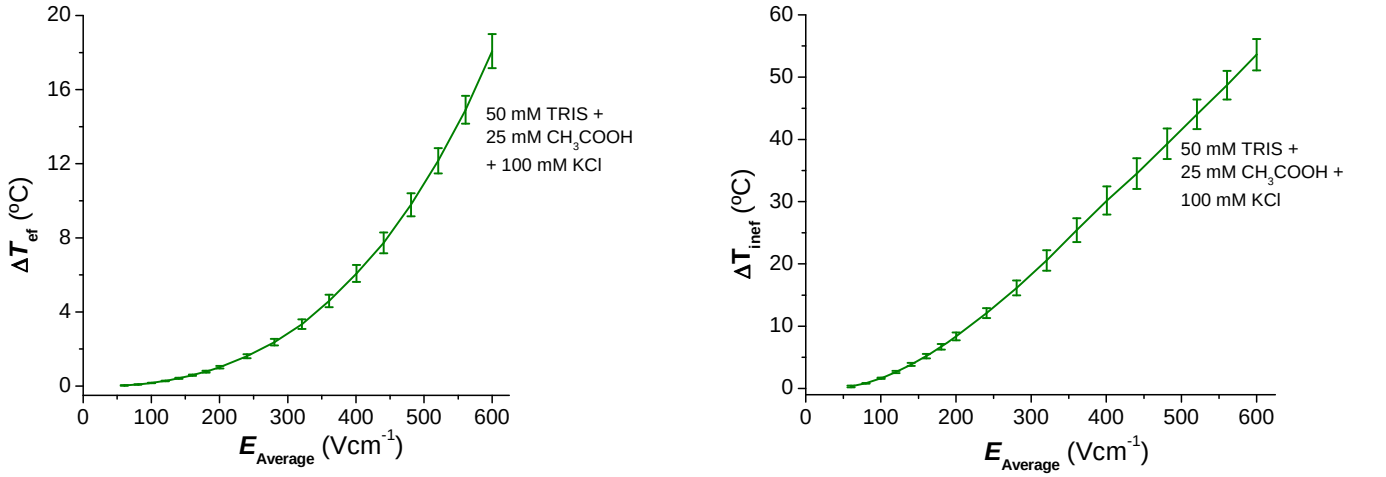

Figure S8: Increase in temperature as a function of the electric field strength in the efficiently-cooled section (**Left**) and inefficiently-cooled section (**Right**) of a 50 µm internal diameter capillary containing 50 mM TRIS + 25 mM CH_3COOH + 100 mM KCl. The coolant temperature was set to 20ºC. Error bars are to ± 2 standard deviations.

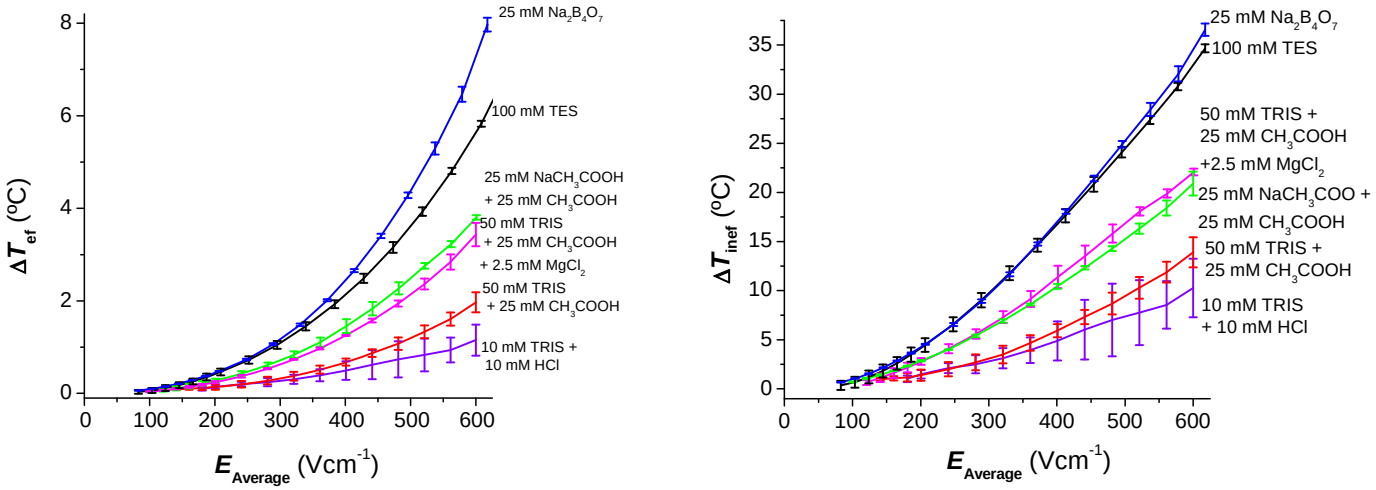

Figure S9: Increase in temperature as a function of the electric field strength in the efficiently-cooled section (**Left**) and inefficiently-cooled section (**Right**) of a 75 µm internal diameter capillary containing various electrolytes. The coolant temperature was set at 20ºC. Error bars are to ± 2 standard deviations.

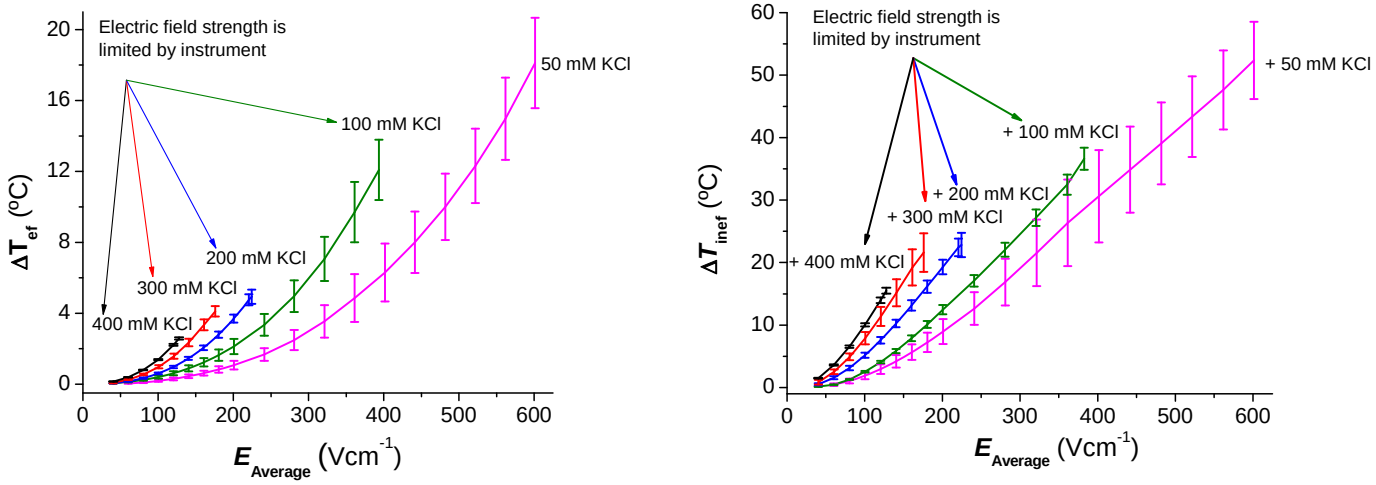

Figure S10: Increase in temperature as a function of the electric field strength in the efficiently-cooled section (**Left**) and inefficiently-cooled section (**Right**) of a 75 µm internal diameter capillary containing 50 mM TRIS + 25 mM CH_3COOH with varying concentrations of KCl. The coolant temperature was set to 20ºC. Error bars are to ± 2 standard deviations.

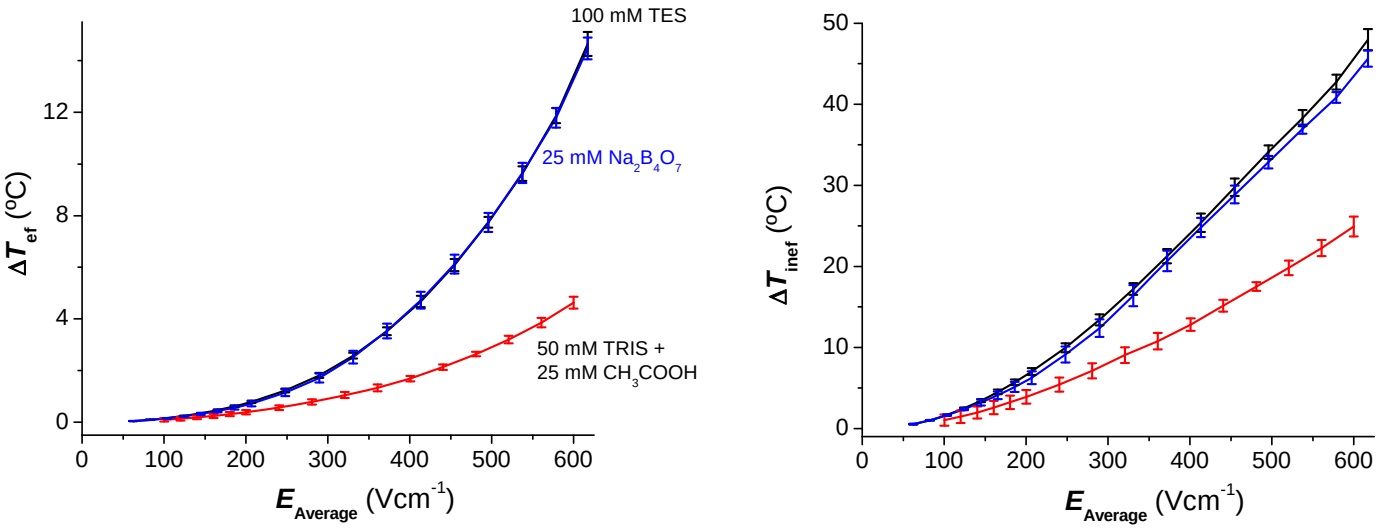

Figure S11: Increase in temperature as a function of the electric field strength in the efficiently-cooled section (**Left**) and inefficiently-cooled section (**Right**) of a 100 µm internal diameter capillary containing various electrolytes. The coolant temperature was set at 20ºC. Error bars are to ± 2 standard deviations.

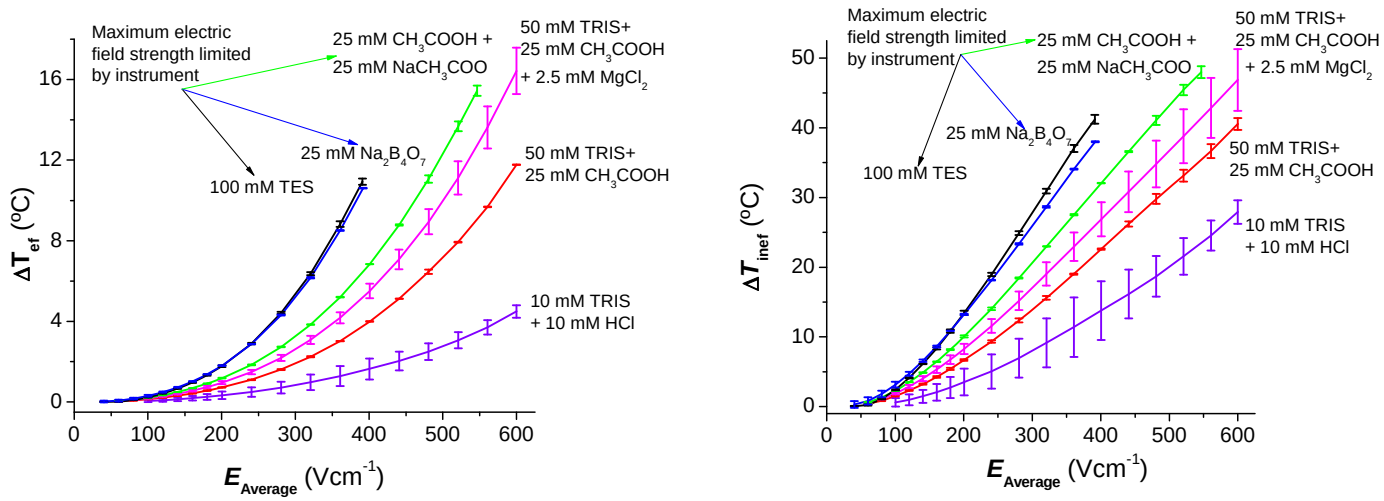

Figure S12: Increase in temperature as a function of the electric field strength in the efficiently-cooled section (**Left**) and inefficiently-cooled section (**Right**) of a 150 µm internal diameter capillary containing various electrolytes. The coolant temperature was set at 20ºC. Error bars are to ± 2 standard deviations.

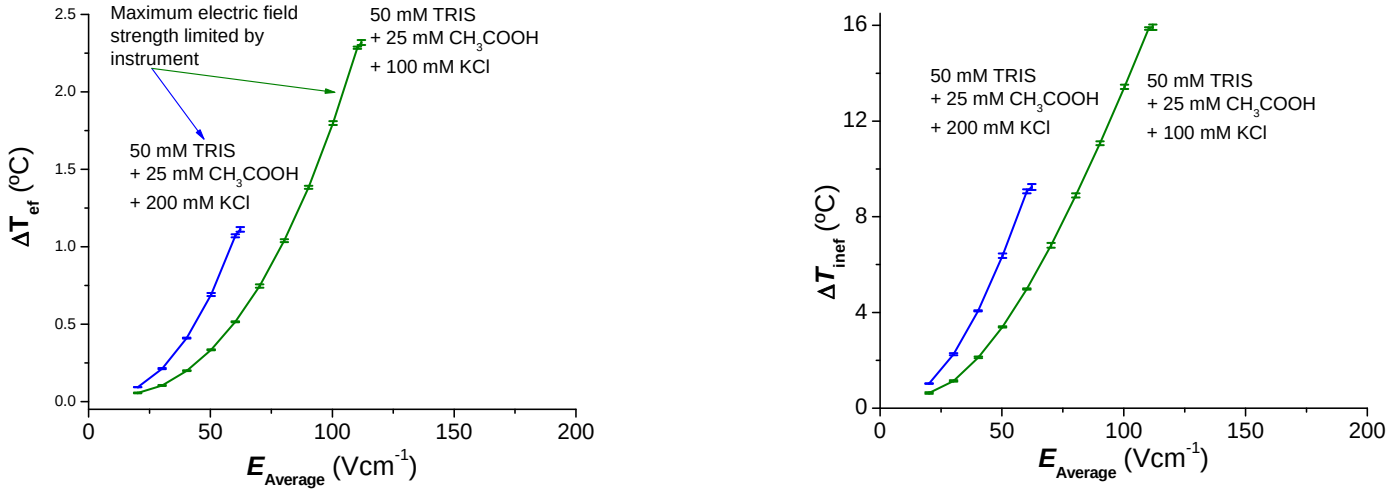

Figure S13: Increase in temperature as a function of the electric field strength in the efficiently-cooled section (**Left**) and inefficiently-cooled section (**Right**) of a 150 µm internal diameter capillary containing 50 mM TRIS + 25 mM CH_3COOH with varying concentrations of KCl. The coolant temperature was set to 20ºC. Error bars are to ± 2 standard deviations.

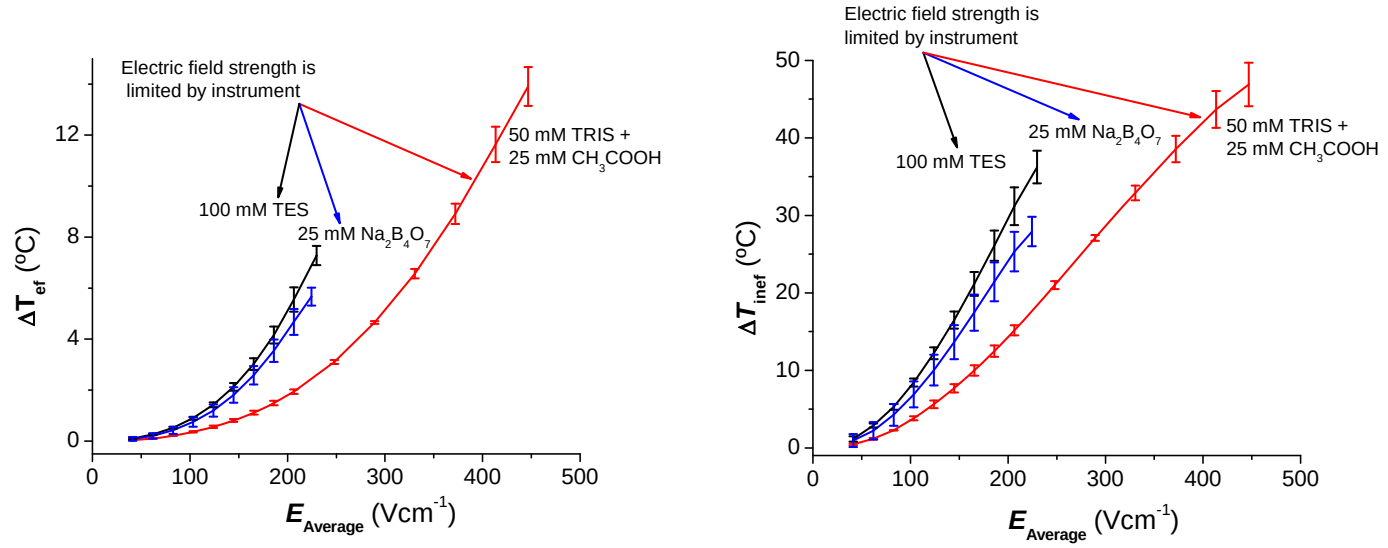

Figure S14: Increase in temperature as a function of the electric field strength in the efficiently-cooled section (**Left**) and inefficiently-cooled section (**Right**) of a 200 µm internal diameter capillary containing various electrolytes. The coolant temperature was set at 20ºC. Error bars are to ± 2 standard deviations.

References

(1) Evenhuis, C. J.; Musheev, M. U.; Krylov, S. N. *Anal. Chem.* **2010**, *82*, 8398-8401.
(2) Knox, J. H.; McCormack, K. A. *Chromatographia* **1994**, *38*, 207-214.
(3) Nishikawa, T.; Kambara, H. *Electrophoresis* **1996**, *17*, 1115-1120.
(4) Petersen, N. J.; Nikolajsen, R. P. H.; Mogensen, K. B.; Kutter, J. P. *Electrophoresis* **2004**, *25*, 253-269.
(5) Evenhuis, C. J.; Haddad, P. R. *Electrophoresis* **2009**, *30*, 897-909.
(6) Andersson, S. P.; Andersson, O.; Backstrom, G. *Int.J.Thermophys.* **1997**, *18*.
(7) Hruska, V.; Evenhuis, C. J.; Guijt, R. M.; Macka, M.; Gas, B.; Marriott, P. J.; Haddad, P. R. *Electrophoresis* **2009**, *30*, 910-920.